

Blast Algorithm Development: Definition of Modified Blast Algorithms for PBX Based Explosives

Jim Dunnett^{*}, Dennis Flynn^{**} and James Wharton^{**}

^{*} Fluid Gravity Engineering, 83 Market Street, St Andrews, Fife KY16 9NX, United Kingdom

^{**} BAE Systems, Land Systems, Central Avenue, Chorley, Lancashire PR7 6AD, United Kingdom

Abstract

A recent series of experiments was performed to examine the effects metal cases have in diminishing the blast from an explosive charge. The trials programme was selected to study this case effect for both ideal and non-ideal charge types, and for two different case materials. The experimental set-up used and the analysis of the pressure gauge data obtained are both described. The results show that the case effect depends on both the charge type and case material. Moreover, it is seen that, for each particular system, the observed effects are well fitted using a generalised form of the Fisher algorithm.

This work was performed by BAE Systems, Land Systems and Fluid Gravity Engineering in support of the ongoing Warheads 2 programme. The work was sponsored by RAO-WPE as part of UK MoD technology investment programmes.

Introduction

Surrounding a charge with a metal case has the effect of reducing the strength of the resulting blast. Historically, a number of algorithms have emerged that attempt to quantify this 'case effect' (see table 1). In each of these, the blast reduction is specified in terms of an effective bare charge mass M_{EBC} - the mass of bare charge required to produce the same blast as the cased system. (It is noted that none of these algorithms makes any distinction between the two key measures of blast strength: peak impulse and peak pressure. It is presumed that they are intended to apply equally to both). Algorithms like these are useful tools, allowing blast performance to be estimated without recourse to expensive experimentation or complicated hydrocode modelling. Figure 1 shows the case effects predicted using these existing algorithms. It is noted that there is little consensus here; different algorithms predict significantly different effects. Moreover, with the exception of the Fisherⁱ algorithm, the origins of these algorithms have become largely obscure, so that it is not possible to make an informed judgement as to which is the best suited to any given system or how relevant they are to modern choices for charge type and case material.

While some data on measured case effects is available in the literature (e.g. Grime and Sheardⁱⁱ, Heinemann *et al*ⁱⁱⁱ and Filler^{iv}), overall this is sparse, providing an insufficient basis upon which to either judge the suitability of existing algorithms or develop new ones.

It was against this background that it was decided to generate a new dataset of case effects results, by performing a fresh series of experiments - one for which the design and set-up was well understood.

Fano:	$\frac{M_{EBC}}{M_{charge}} = 0.2 + \frac{0.8}{1 + 2 \frac{M_{case}}{M_{charge}}}$
Modified Fano:	$\frac{M_{EBC}}{M_{charge}} = 0.6 + \frac{0.4}{1 + 2 \frac{M_{case}}{M_{charge}}}$
Warren:	$\frac{M_{EBC}}{M_{charge}} = 0.4 + \frac{0.6}{1 + 2 \frac{M_{case}}{M_{charge}}}$
Fisher:	$\frac{M_{EBC}}{M_{charge}} = 0.2 + \frac{0.8}{1 + \frac{M_{case}}{M_{charge}}}$
Modified Fisher:	$\frac{M_{EBC}}{M_{charge}} = 0.6 + \frac{0.4}{1 + \frac{M_{case}}{M_{charge}}}$

Table 1 Existing case-effect algorithms

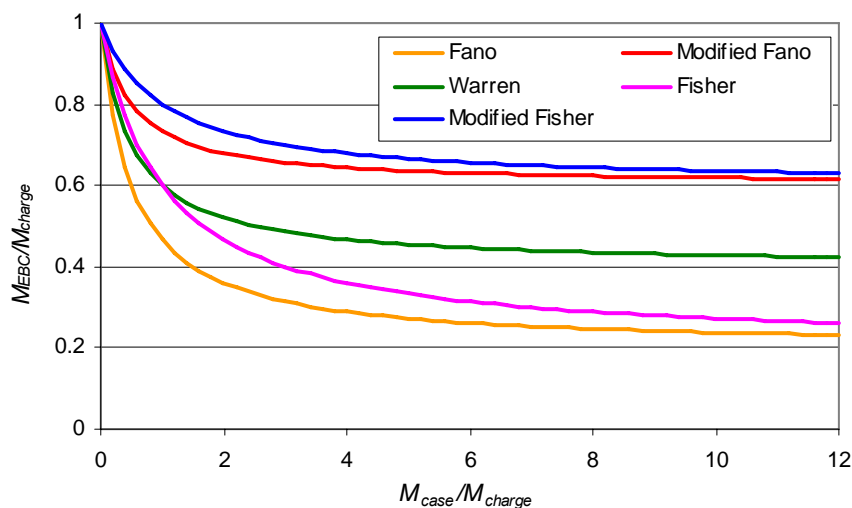


Figure 1 Effects computed using existing algorithms

Experimental programme

The programme was chosen to allow case effect measurements to be made for two different case materials and for systems containing both ideal and non-ideal charge types. (Here a non-ideal explosive is defined as one in which a significant fraction of the energy release occurs behind the Chapman-Jouguet plane). Aluminium 6086T6 alloy and EN24 steel were chosen as the two case materials. These metals were selected because of their contrasting fracture mechanics, with the aluminium having a relatively high ductility, while the steel is expected to be more brittle. ROWANEX 1100 (RX1100 – 88% RDX, 12% plasticiser/binder) and ROWANEX 1400 (RX1400 – 66% RDX, 22% aluminium, 12% plasticiser/binder) were selected as the ideal and non-ideal explosive types, respectively.

Table 2 lists the numbers of firings completed, to date, for the various charge/case configurations.

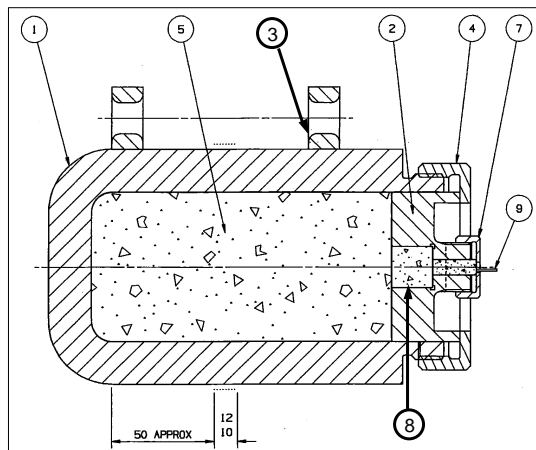
	RX1100	RX1400
Bare charge	3	3
Steel case	0.5kg	2
	2kg	2
	5kg	1
	10kg	2
Aluminium case	0.5kg	2
	2kg	2

Table 2 Matrix of completed experiments

Experimental design and set-up

Figure 2 shows the charge/case design used in these experiments. A single-end initiated cylindrical design was selected because it was relatively simple to manufacture and to work with experimentally. The charge has an L/D ratio of 2 and a nominal mass of 1kg. Case and endplate designs are chosen to ensure, as far as possible, a constant thickness of metal surrounding the charge.

Typical Charge Configuration



Note: - Case thickness chosen to achieve correct case mass to charge mass ratio



- 1 - Fragmenting Case
- 2 - Charge closure
- 3 - Lifting eyelets
- 4 - Clamp Ring
- 5 - Charge (nominally 1kg mass, 2:1 L/D)
- 7 - Detonator Clamping Ring
- 8 - Booster Pellet (20x20 Debrix 18AS)
- 9 - Range Detonator (RP80)

Figure 2 Charge design

Each experiment was fired with the charge suspended 2m above the ground and its axis horizontal. Blast pressures were recorded using a combination of B12 and ICP gauges. These were mounted 2m above ground, on poles positioned along a line perpendicular to the charge's axis. The gauges were positioned to record blast

pressures 3m, 4.5m, 6m and 10m from the charge, with two gauges at each position one mounted above the other. This set up (and the positioning of additional instrumentation, not discussed here) is illustrated in figure 3.

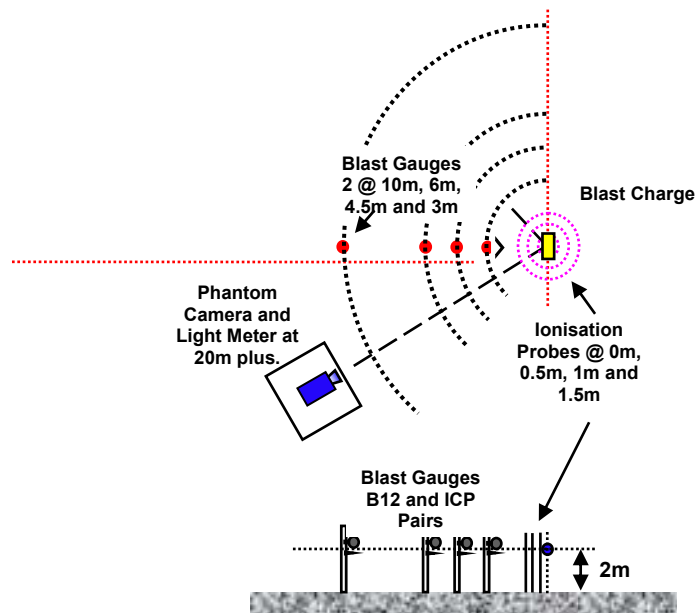


Figure 3 Layout of gauges (and other instrumentation)

Results and analysis

As an example of the records obtained in these experiments, figure 4 shows pressures measured at the 6m gauge position from an RX1100 shot with a 2kg steel case. The high level of noise seen here is a common feature of the results from cased rounds. It is noted that in each of the records the noise starts some time before the arrival of the blast wave. Comparisons with simple code models have shown that the timing of these precursor features correlate with predicted fragment propagation times, leading to the presumption that the noise is due to signals (bow waves) from case fragments passing within the vicinity of the gauges.

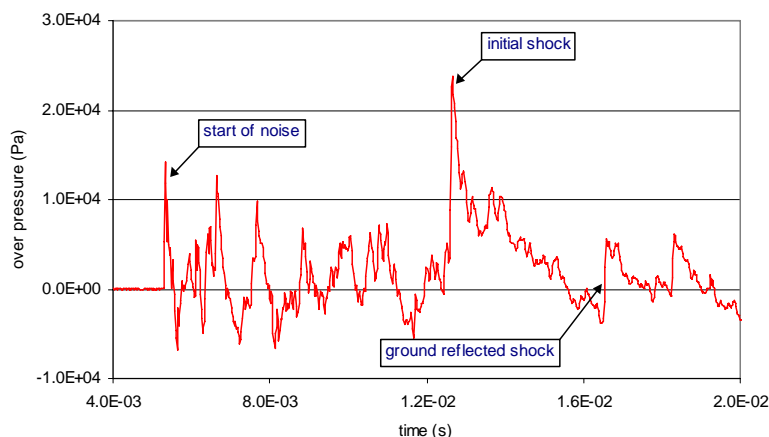


Figure 4 Pressure recorded at upper gauge position, 6m from RX1100 charge with 2kg steel case

Because of this high level of noise, it was not possible to obtain accurate assessments of peak blast pressures from the cased charge experiments. Consequently, it was not possible to determine the effect the case has on peak pressure, directly from these experiments. Instead, the results were used to determine peak impulses.

Figure 5 shows the impulse determined by integrating the figure 4 pressure plot, starting from the time at which the initial shock arrives. It had been intended that these experiments would be used to determine case effects on free-field blast, i.e. excluding any additional effects due to reflected waves. In the example shown, peak impulse is reached shortly before the arrival of the ground reflected shock. On other 6m gauge readings – particularly those obtained at the lower pole positions - the ground reflected shock arrives before peak impulse is reached, although only marginally so. Where the ground reflected shock did arrive ‘early’, it was possible to adjust the 6m gauge results by taking the decline in pressure immediately prior to the arrival of the reflected shock and projecting this on to estimate the peak impulse which would have been achieved in the absence of the reflected shock.

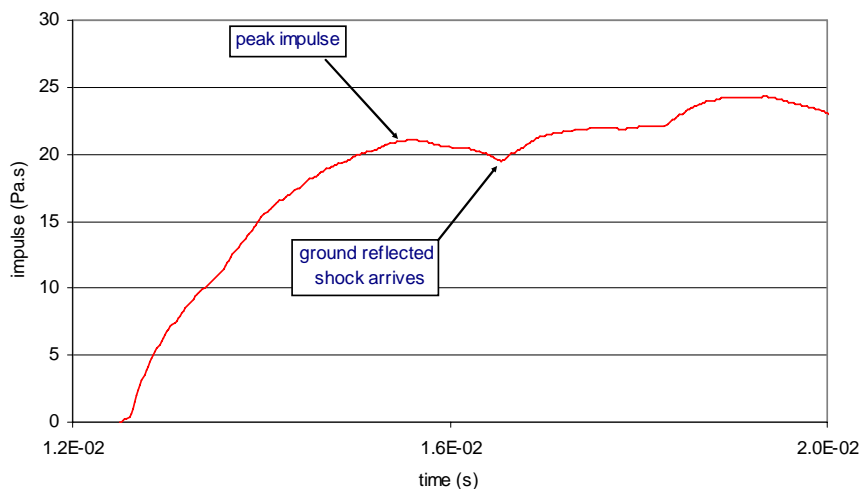


Figure 5 Positive impulse at upper gauge position, 6m from RX1100 charge with 2kg steel case

However, as is illustrated by the result shown in figure 6, at the 10m gauge positions the ground reflected shock arrives well before peak impulse is achieved. It was felt that the extrapolation required to infer peak impulse figures from these results would introduce unacceptably large uncertainties. Consequently, the 10m results were ignored and only the 3m, 4.5m and 6m results were used to determine the case effects on impulse. (Indeed, in later firings the 10m gauge position was abandoned with the gauges moved to provide additional results at the 4.5m position).

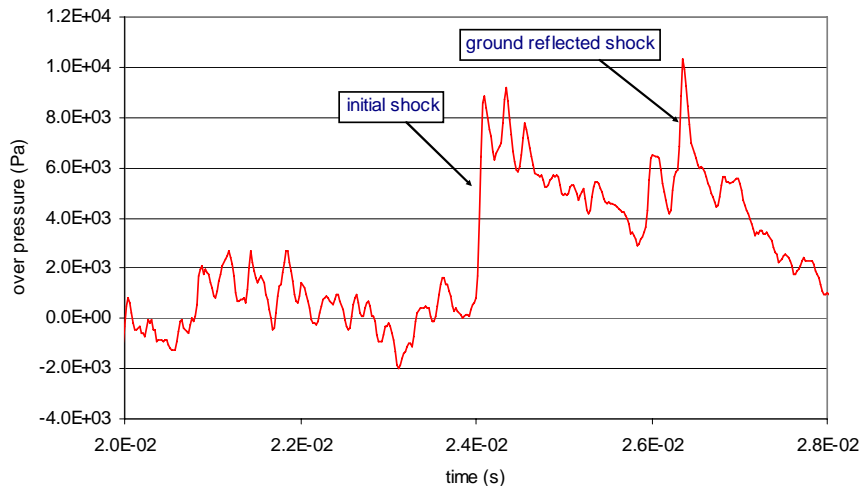


Figure 6 Pressure recorded at upper gauge position, 10m from RX1100 charge with 2kg steel case

Figure 7 shows the peak impulse results determined from RX1100 bare charge and steel cased experiments. These results were obtained by averaging across all the results for each case/charge configuration. It is seen from the plot that the case acts to reduce the impulse from the blast - the heavier the case, the lower the impulse.

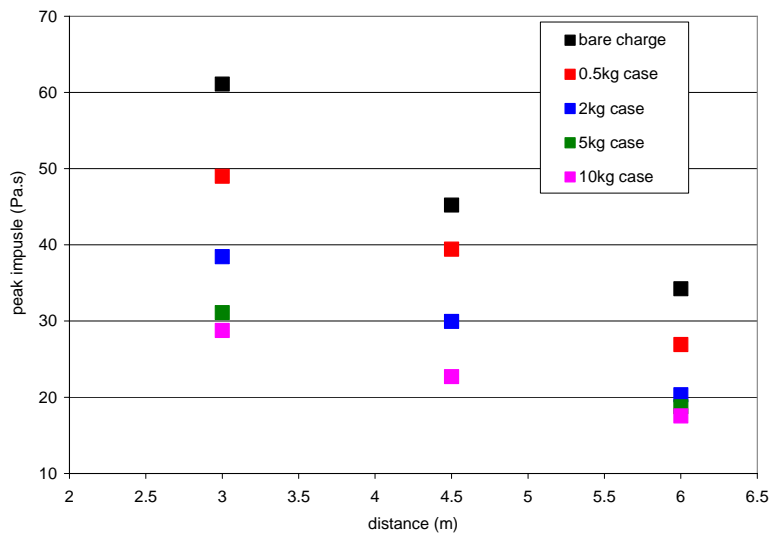


Figure 7 Peak impulses measured for RX1100 charges with steel cases

Case effects

As noted, it is customary to express case effects in terms of a reduction in effective bare charge mass. In order to determine these case effects, the impulse results are first expressed as equivalent masses of some reference explosive. Thereafter the case effect is obtained simply by taking the ratio of the equivalent mass determined from the cased result to that obtained from the corresponding bare RX1100 result.

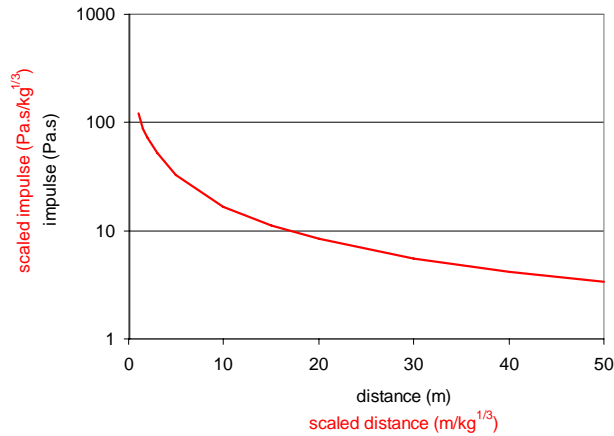


Figure 8 Peak impulses computed for 1kg spherical TNT charge

Figure 8 shows a plot of peak impulse as a function of distance, as computed for a 1kg spherical TNT charge. In the calculation the TNT is treated as an ideal explosive (i.e. CJ detonation is assumed), so that the results scale hydrodynamically. That is, the plot may be generalised so that it applies to any mass of (bare, spherical) TNT charge, simply by plotting scaled impulse against scaled distance. Scaled impulse i_{scl} and scaled distance r_{scl} are computed as,

$$i_{scl} = \frac{i}{\sqrt[3]{M_{charge}}}$$

$$r_{scl} = \frac{r}{\sqrt[3]{M_{charge}}}$$

Using this generalised plot, any subsequent $i(r)$ result can be interpreted as an equivalent bare mass of TNT simply by finding the mass M_{EBC} such that the point

$$\left(\frac{r}{\sqrt[3]{M_{EBC}}}, \frac{i}{\sqrt[3]{M_{EBC}}} \right)$$

lies on the plot. Proceeding in this fashion the RX1100 bare charge and steel cased impulse results were converted to bare charge masses and case effects computed.

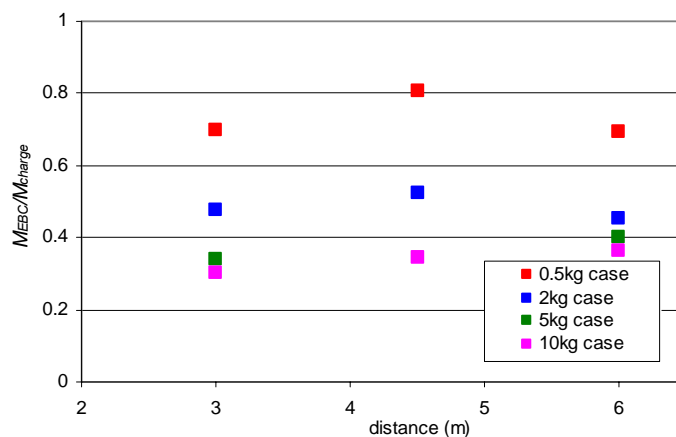


Figure 9 Case effects inferred from RX1100/steel case impulse results

Figure 9 shows case effects determined for the RX1100/steel systems. Although some variation with distance is seen, there is no clear trend, and it is assumed that these are simply random variations due to experimental uncertainties. Accordingly, a single effect figure is computed for each case mass, by averaging across the three gauge positions. Figure 10 shows the resulting plot of case effect as a function of case mass for RX1100/steel systems.

It is noted that the Fano, Modified Fano and Warren algorithms are each specific examples of a generalised (Fano) form,

$$\frac{M_{EBC}}{M_{charge}} = \alpha + \frac{(1-\alpha)}{\left(1 + \frac{2M_{case}}{M_{charge}}\right)}$$

Likewise, the Fisher and modified Fisher algorithms are specific examples of a generalised Fisher form,

$$\frac{M_{EBC}}{M_{charge}} = \beta + \frac{(1-\beta)}{\left(1 + \frac{M_{case}}{M_{charge}}\right)}$$

Treating α and β as free parameters, both these forms were fitted (in a 'least squares' sense) to the RX1100/steel case effects data. These fitted curves are shown in figure 10. It is noted that the Fisher form, in particular, fits the data very well.

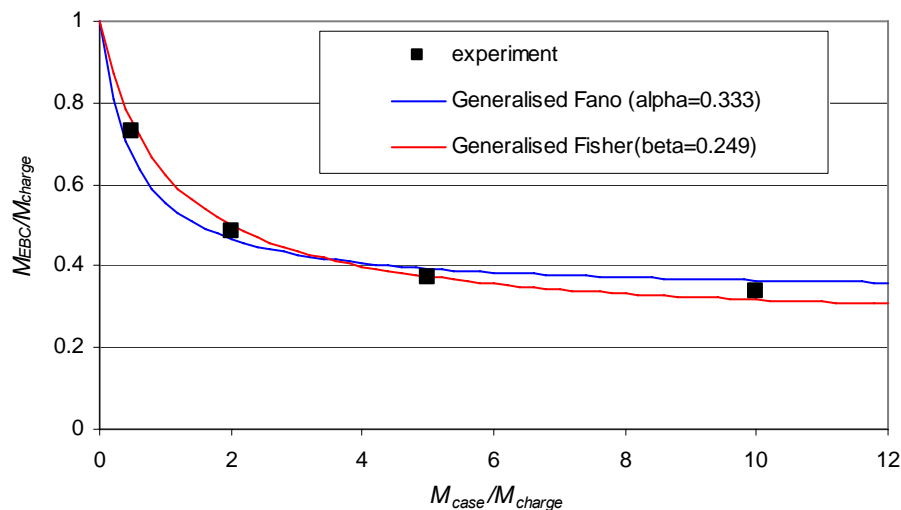


Figure 10 Case effects as a function of case mass for RX1100/steel case systems

Other systems

The analysis described above was repeated to determine case effects for the RX1100/aluminium, RX1400/steel and RX1400/aluminium cased systems. The effects determined for each of these systems are plotted in figure 11. Again, both the generalised Fano and Fisher functions were fitted to the data for each system. It

was found that the Fisher form gave a consistently better fit to the data than the Fano form. These fitted Fisher curves are plotted (solid lines) in figure 11. Table 3 lists the β parameters used to fit the Fisher algorithm to the case effects data for each system.

From the results shown it is immediately obvious that the case effect depends on both case material and charge type. A case has much less of an effect in diminishing the blast from an RX1400 charge compared to a RX1100 one. Although, the case effect is seen to be dependent on case material, the material dependence appears to depend on charge type. For an RX1100 charge there is a greater case effect from steel cases compared to aluminium ones, while for RX1400 charges aluminium cases show the greater effect.

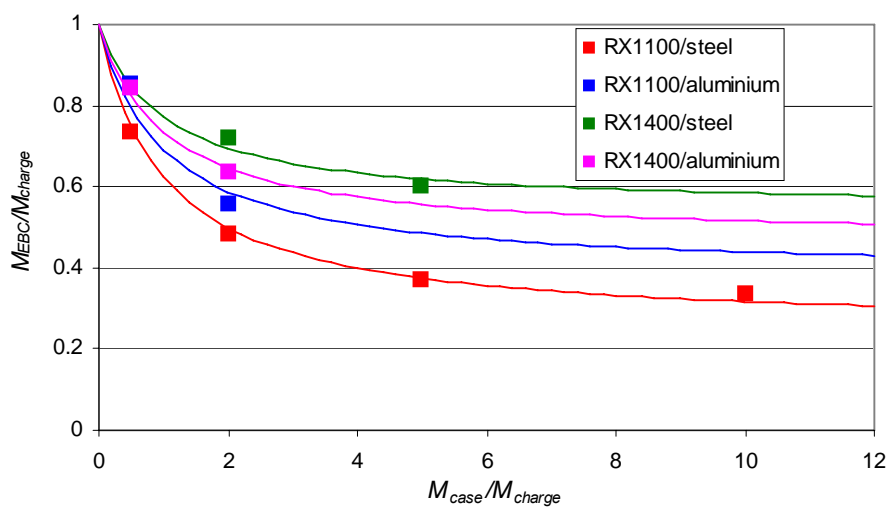


Figure 11 Case effects as a function of case mass for different charge/case systems together with fitted Fisher curves

System	β
RX1100/steel	0.249
RX1100/aluminium	0.383
RX1400/steel	0.543
RX1400/aluminium	0.468

Table 3 Values of Fisher parameter β fitted to case effects for different systems

Summary and Conclusions

A set of experiments has been performed to measure case effects for four different systems. The results obtained show that, as well as the mass of the case, the case effect depends on the charge type and case material. At this stage, the reasons behind this charge and case material dependence are not well understood and are being investigated using code models. These experimental results will act as a key input to this study.

Case effects algorithms have been developed to fit the experimental results, based on generalised forms of the Fano and Fisher curves. It is found that the Fisher form gives the consistently better fit to the data.

It is noted that there is a degree of random variation in the impulse results obtained from the experiments and it is presumed that the case-effect results presented may be subject to large uncertainties, although no rigorous error analysis has been performed. Ultimately, the key to reducing these uncertainties is to perform multiple repeat experiments, to improve the statistical basis of the study. However, even with the simple set-up used in these experiments, this would be time-consuming and costly. At this point plans for future experimental work are limited to, firstly, measuring case effects for a third explosive type - PBX N109 - and, secondly, filling in some important gaps in the current dataset. In particular, there are plans to fire RX1100 and RX1400 charges with 10kg aluminium cases and RX1400 charges with 10kg steel cases. It has been recognised that if, as appears to be the case, case effects are generally well fitted using a Fisher type algorithm, then the underlying algorithm will be most accurately established using results obtained with high M_{case}/M_{charge} ratios.

References

- ⁱ Fisher E.M, Aronson C.J, “The effect of the steel case on the air blast from high explosives”, NAVORD report 2753, (1953)
- ⁱⁱ Grime G, Sheard H, “The experimental study of blast from bombs and bare charges”, Proc. Roy. Soc. Vol. 187(1944)
- ⁱⁱⁱ Heinemann R, Snook R, Stein S, “The effects of casing materials and explosive compositions on blast”, Picattiny Arsenal Technical Report, DR-TR 1-60 (1961)
- ^{iv} Filler W.S, “The Influence of inert cases on air blast: an experimental study”, Proceedings 6th Detonation Symposium (1976)